ECS Transactions, 11 (7) 91-101 (2007)
10.1149/1.2779073 ©The Electrochemical Society

In-situ FTIR Study of Atomic Layer Deposition (ALD) of Copper Metal Films

Min Dai[a], Jinhee Kwon[a], Erik Langereis[a], Leszek Wielunski[a], Yves J. Chabal[a]
Zhengwen Li[b], and Roy. G. Gordon[b]

[a] Laboratory for Surface Modification, Department of Physics and Astronomy, Rutgers University, Piscataway, New Jersey 08854, USA
[b] Department of Chemistry and Chemical Biology, Harvard University, Cambridge, Massachusetts 02138, USA

Growth mechanisms of atomic layer deposition of copper films on various substrates using a novel metal precursor $[Cu(^{s}Bu\text{-}amd)]_2$ and molecular H_2 are investigated by *in-situ* transmission Fourier transform infrared spectroscopy (FTIR). The Cu-precursor reacts with SiO_2 and Al_2O_3 surfaces by forming chemical bonds with the surface. Upon reduction by H_2, Cu atoms agglomerate, yielding additional reactive sites for more Cu-precursors. Cu agglomeration is relatively weaker on nitrided Si surfaces. H-terminated Si surfaces show a minimal reaction with the Cu precursor. The growth rates of the Cu films on all these surfaces are all less than 1 Å per cycle.

Introduction

Copper is replacing aluminum in the microelectronics because of its superior electrical conductivity (1). For such microelectronics applications, a controlled method to deposit uniform and conformal thin copper films is required. ALD is a very promising method and shows great advantages in depositing uniform and conformal films with high purity (2, 3). In the past two decades, it has been widely and successfully utilized to deposit metal oxides and nitrides. However, the potential applications of ALD to deposit pure metals have been limited by the lack of efficient precursors with high volatility, thermal stability and reactivity (4). A precursor should have a high enough vapor pressure to release enough material during each ALD cycle but not too high to prevent fast recovery after the reactor is exposed (5). It must be stable at the growth temperature without decomposition or degradation over long periods of time. Moreover, real applications require thorough and fast reactions with other oxidizing (or reducing) precursors with little contamination in the films.

Recently, R. G. Gordon et al. reported ALD grown Cu films with high conformality and conductivity even inside a hole with aspect ratio over 35:1 by using a novel liquid precursor Copper (I) di-sec-butylacetamidinate ($[Cu(^{s}Bu\text{-}amd)]_2$) (9). Its equilibrium vapor pressure is as high as 0.23 Torr at 95°C. Another advantage of this precursor is that it is reduced by molecular H_2 at relatively low temperature (<200°C) which is favorable to deposit smooth and continuous pure thin copper layer. It also readily reacts with water and NH_3 to deposit copper oxide or copper nitride.

In-situ characterization during ALD film growth is particularly important to understand the interaction of new precursors with technologically important surfaces. We utilized FTIR to monitor the reaction of $[Cu(^{s}Bu\text{-}amd)]_2$ with various surfaces (SiO_2, Al_2O_3, nitrided and H-terminated Si) and the effect of subsequent molecular H_2 exposures. *Ex situ* RBS measurements were also performed to determine the Cu coverage, and hence the growth rate.

Experiments

All the experiments are done in a home-made ALD system. Fig. 1 shows the schematic of the ALD reactor with a Thermo Nicolet 670 interferometer and a MCT/B detector for *in-situ* FTIR measurements. A single-pass transmission geometry is adopted with an incidence angle close to the Brewster angle to maximize transmission, minimize interference, and increase sensitivity to absorptions below ~1500 cm^{-1}.

Various substrates are prepared from double side polished, float zone grown and lightly doped (~10 Ω·cm) Si (100) and Si (111) wafers passivated by native oxide. All samples are rinsed in acetone and methanol, and cleaned by a standard RCA treatment to remove organic and metallic contaminants. Hydrogen-terminated Si(100) surfaces are prepared by ~30 seconds HF (~20%) etching at room temperature. For H/Si (111) an additional ~2.5 min NH_4F (~49%) etching is performed afterwards. The samples are then loaded in the ultra pure N_2 purged ALD chamber immediately.

Thermal nitridation is performed by exposing an H/Si (100) substrate to NH_3 gas [99.999%, with Aeronex hydride gas purifier (oxygen and non-methane hydrocarbons impurity <1 ppb)] at 600°C. The exposure time is 2 min at ~8 Torr. The heating and cooling process are both done in NH_3 ambient. Prior to nitridation, the H/Si (100) sample is exposed to NH_3 at a moderate temperature (~150 °C) for 4 min to minimize the physisorption of residual water and other contamination on the surface.

Al_2O_3 growth is achieved by introducing TMA and D_2O pulses alternatively into the ALD chamber. A thin (~10 Å) layer of Al_2O_3 (10 ALD cycles) is deposited on a H/Si (111) surface. Both TMA and D_2O are kept at room temperature, using their vapor pressures to deliver them into the chamber without a carrying gas. The substrate is kept at 300°C during the deposition. We use D_2O instead of H_2O to avoid interference of environmental H_2O effect on IR measurements. After each precursor exposure, the ALD chamber is well purged and pumped with purified N_2 to prevent gas phase reactions between residual precursors. During film deposition, the reactor pressure (typically ~2-3 Torr for both TMA and D_2O) is monitored with a Baratron (MKS). The pulse lengths are 5s for TMA and 2s for D_2O.

The copper film is deposited by introducing $[Cu(^{s}Bu\text{-}amd)]_2$ and H_2 (99.999%, with Aeronex gas purifier) alternatively into the ALD chamber for *in situ* characterization of the film growth on the differently functionalized Si surfaces. The substrate temperature is kept at 185°C for optimum copper deposition. Purified N_2 is used as the carrier gas to deliver the copper metal precursor. To generate a high enough vapor pressure, the precursor is kept at ~100°C. After each half cycle, the ALD chamber is purged thoroughly and pumped with purified N_2. During film deposition, the pressure of the

copper precursor is around 2 Torr and that of H_2 is >11 Torr. The pulse lengths for the copper precursor and H_2 gas are 2s and 100s, respectively.

The thickness of the ALD-grown copper films is measured by RBS, assuming that the copper film density is equal to the density of bulk copper (8.96 g/cm^3, or 8.49×10^{22} atoms/cm^3).

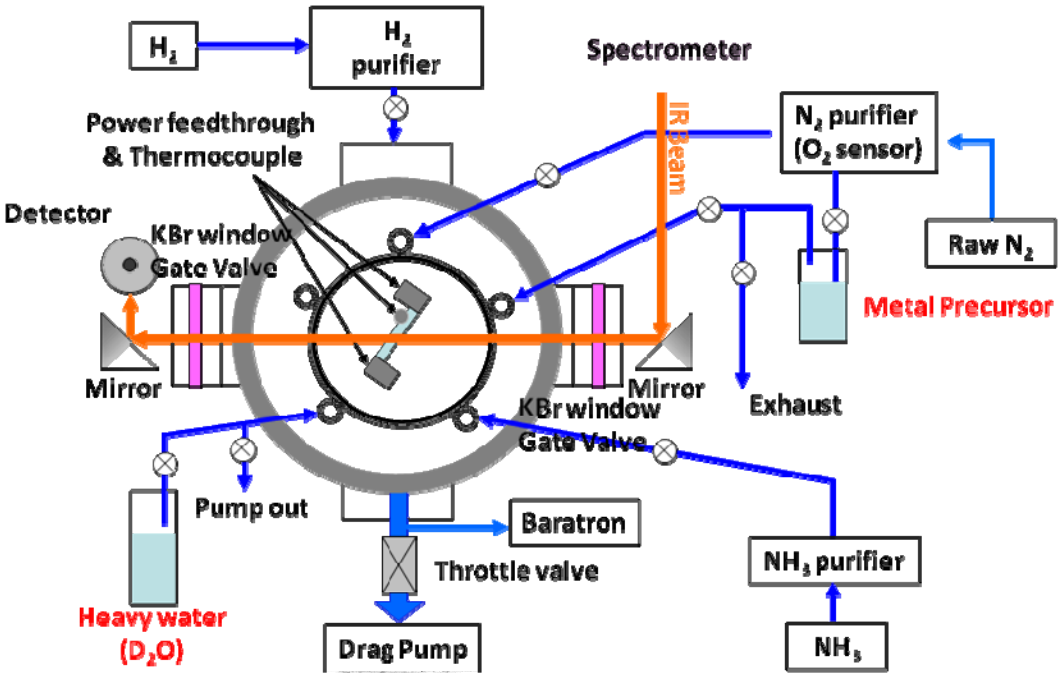

Fig. 1 Schematic diagram of the ALD system for *in situ* FTIR transmission measurements. KBr windows are used and protected by gate valves during the deposition.

Results

Gas phase FTIR measurement of [Cu(^{s}Bu-amd)]$_2$

The chemical structure of the copper precursor [Cu(^{s}Bu-amd)]$_2$ is shown by the inset of Fig. 2. The major advantages of this precursor are that it can react with molecular H_2 at relatively low temperature (< 200^{o}C), its melting point is quite low (~ 77^{o}C), and its evaporation rate is reasonably fast (38 nmol/cm^{2}min at 100^{o}C). Moreover, it is very stable, which makes it a very promising precursor for copper ALD deposition.

Before depositing copper, the [Cu(^{s}Bu-amd)]$_2$ gas phase IR spectrum is measured to determine the composition of the gas prior to reaction. As shown in Fig. 2, this precursor is characterized by CH_3 symmetric (2971 cm^{-1}) and asymmetric (2882 cm^{-1}) stretching modes, CH_2 symmetric (2932 cm^{-1}) and asymmetric (2861 cm^{-1}) stretching modes, a CH_3 symmetric bending mode at 1377 cm^{-1}, and a -NH stretching mode at 3456 cm^{-1}. The

NCN-related ligand modes and the other CH_x bending and deformation modes are in the range of 1000-1600 cm^{-1}. The very strong and sharp feature at 1664 cm^{-1} cannot be assigned to any mode (e.g. NCN stretch) of the ligand bonded to the metal (Cu) center. Instead, it is characteristic of a C=N stretching mode in the free -HNC=N- molecule produced by partial hydrolyzation of the parent precursor molecule, most likely due to a small amount of residual water in the ALD chamber.

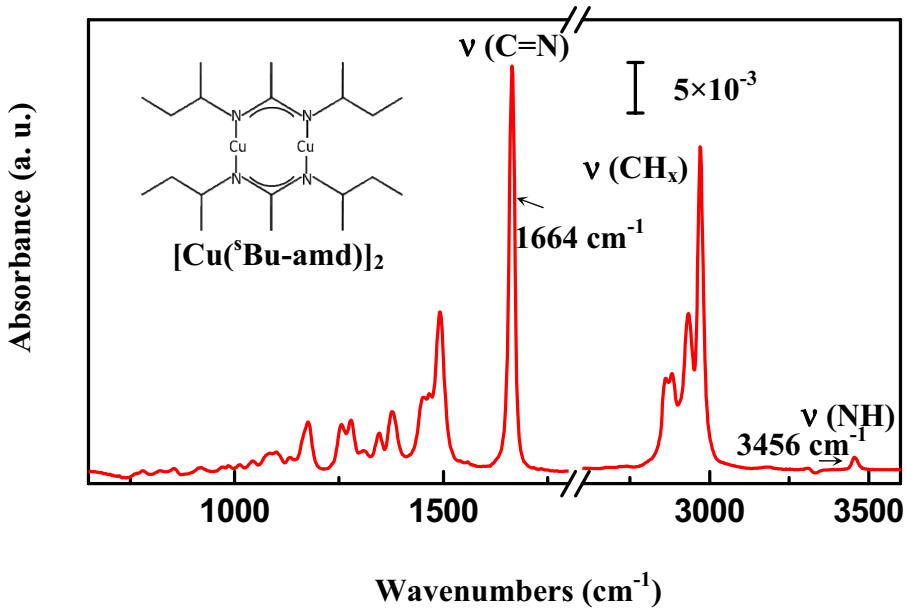

Fig. 2 Gas phase FTIR absorption spectrum of the copper precursor $[Cu(^{s}Bu\text{-}amd)]_2$ used in this study (Partial pressure ~0.4 torr , IR path length ~6 inch). Its chemical structure is shown on the upper left corner (inset).

H/Si (100) surface

H/Si (100) is the most widely used surface in microelectronics. We first examined the reaction between $[Cu(^{s}Bu\text{-}amd)]$ and the HF etched Si (100) surface. Fig. 3 shows the differential absorption spectra of H/Si (100) exposed by $[Cu(^{s}Bu\text{-}amd)]$ precursor at 185°C. Each spectrum is referenced to that recorded after the previous treatment to highlight changes occurring after each processing step (2s exposure to $Cu(^{s}Bu\text{-}amd)$ each time). In total, an integrated exposure of 6s was performed, making it possible to investigate whether surface saturation could be obtained.

As shown in Fig. 3, the initial H/Si (100) surface is characterized by Si-H stretching modes centered around 2100 cm^{-1}, with the 2087 cm^{-1}, 2104 cm^{-1} and 2140 cm^{-1} bands being assigned to mono-, di- and tri-hydrides, respectively (10).

By monitoring the intensity of the Si-H stretching band the reactivity of the copper precursor on the surface can be deduced. After the first 2s dosing, the intensity of this Si-H band is decreased by ~ 14%, and only by ~ 21% and ~22% (relative to the original

H/Si surface) after the second (4s) and third exposures (6s), respectively. The change after 4s exposure is negligible according to the differential spectra, suggesting no more chemical bonding formation. These data indicate that saturation is achieved after ~ 4s integrated exposure time. Concurrently, the symmetric stretching modes of CH_3 at 2966 cm^{-1} and CH_2 2926 cm^{-1} are observed after the first dosing of Cu precursor with little intensity increase afterwards. The behavior of Si-H and CH_x stretch modes indicates that most of the surface reaction happens during the first dosing (2-4s exposure). RBS measurements performed after 2 cycles show that the average growth rate is 0.12 Å per cycle.

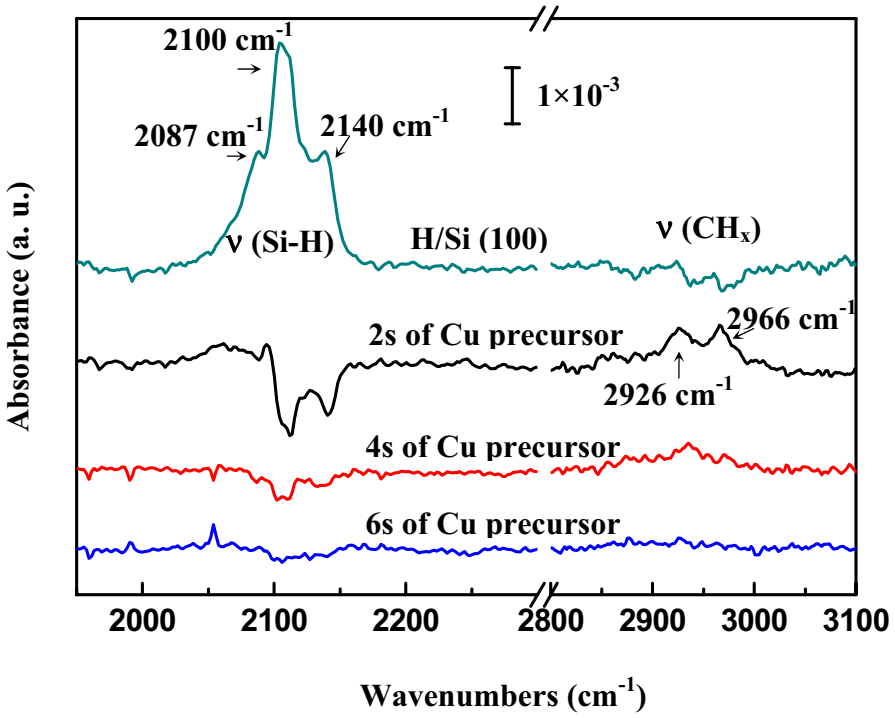

Fig. 3 Differential FTIR absorption spectra of the $[Cu(^{s}Bu\text{-}amd)]_2$ on H/Si (100) surface. Each spectrum is referenced to the spectrum recorded for the previous treatment. The spectrum of H/Si is referenced to that of the oxidized surface; the spectrum of 2s Cu precursor exposure is referenced to that of the H/Si(100) surface; the spectrum of 4s Cu precursor exposure is referenced to that of the 2s Cu precursor exposure, and so on.

SiO_2 surface

In general, an oxidized Si surface is much more reactive to metal precursors than H-terminated Si surfaces. We therefore studied the reactivity of $[Cu(^{s}Bu\text{-}amd)]_2$ with Si(100) covered by a native oxide. Fig. 4 shows the results of a series of cycles (20 in total) performed with the substrate at 185°C, with 2s dosing of $[Cu(^{s}Bu\text{-}amd)]_2$ and 100s dosing of H_2 as described in the experimental part,. The results are again presented in the form of differential absorption spectra.

Upon an initial dosing of [Cu(^{s}Bu-amd)]$_2$ on the oxide surface (0.5 cycle), there is a clear decrease in SiO_x phonon absorption evidenced by two negative peaks centered at 1075 cm^{-1} and 1247 cm^{-1} (TO/LO modes of Si-O-Si) (11). This intensity loss indicates that initially part of the SiO_2 matrix is chemically involved with the precursor. Concurrently, a broad absorption band centered at 1010 cm^{-1} appears, corresponding to the formation of Si-O-Cu bonds. Upon H_2 exposure (1 cycle), there is a partial recovery of the SiO_x phonon modes. The same phenomenon is observed during subsequent cycles, namely after the Cu precursor dosing the SiO_x phonon mode intensity decreases and after the H_2 dosing the SiO_x mode intensity is partially recovered, although the degree is less after each cycle. Even after 18 cycles the same phenomenon is observed, indicating that the SiO_2 is not fully covered with continuous copper film after each full cycle, so that the precursor can still reach and react with oxide surface during the subsequent cycle.

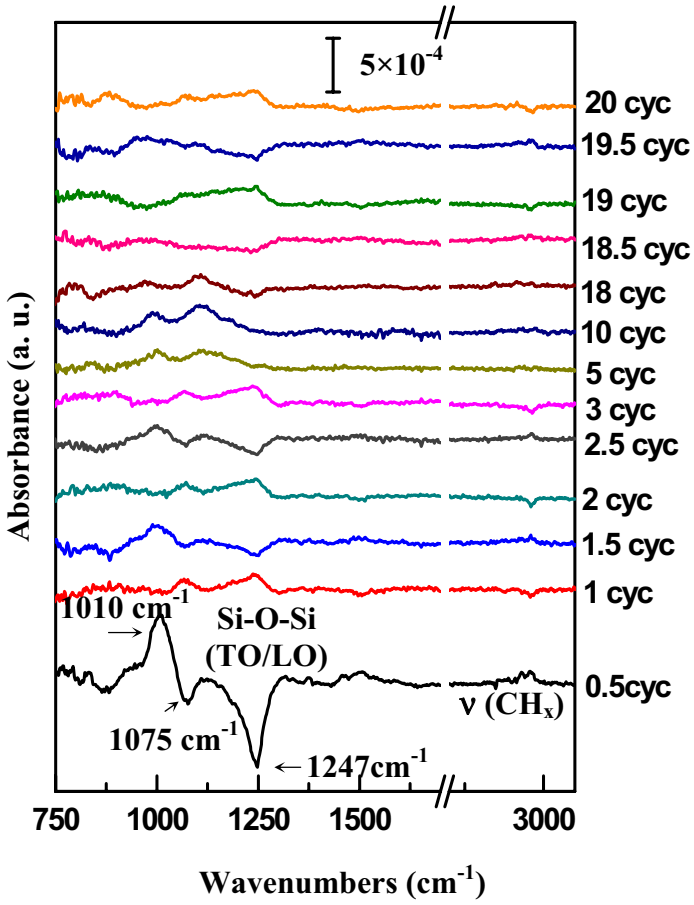

Fig. 4 Differential FTIR absorption spectra of 20 cycles (H_2 dosing after Cu(^{s}Bu-amd)]$_2$) copper ALD on Si oxide. Each spectrum is referenced to that of the surface subjected to the last treatment: oxide surface for the 1st [Cu(^{s}Bu-amd)]$_2$ half cycle, and the resulting surface for the first H_2 dosing, so on and so forth. Each 0.5 cycle is Cu precursor dosing and full cycle is ended by H_2 dosing.

The above observations suggest that after the H_2 dosing, the precursor on the surface is reduced to pure copper atoms that can then diffuse and self-agglomerate to form copper

particles. As they agglomerate, the chemical bonds with the underlying SiO_x surface are broken, partially restoring the initial phonon modes (9) and reactive sites of the original surface. Consequently, the precursor can still reach the oxide surface even after 20 cycles.

It also can be observed that the intensity of CH_x stretching modes at 2800 cm^{-1}- 3000 cm^{-1} increases slightly after each copper precursor dosing, and decreases after H_2 dosing, confirming that the precursor is adsorbed with some of its ligands and the H_2 does react by removing these ligands. The overall intensity of the 2800 cm^{-1}- 3000 cm^{-1} (CH_x stretching modes) and 1200 cm^{-1}-1500 cm^{-1} (CH_x deformation modes) remains very low, suggesting that the carbon contamination in the copper film is low.

The Cu coverage after 20 cycles measured by RBS is 6 Å ($4.7 \times 10^{15}/cm^2$), indicating that the average growth rate of 0.3 Å per cycle. For other similar experiments with only 6- or 7-cycle deposition of copper, the average growth rate is ~ 0.6 Å per cycle, indicating that the precursor is less reactive with copper than silicon oxide. The growth rate deceases after a thin copper film is deposited on the surface, covering most of the oxide.

Al_2O_3 surface

Characterizing Cu deposition on Al_2O_3 is also important for the fabrication of gate stacks for future microelectronic applications. Fig. 5 summarizes the results obtained on a thin Al_2O_3 film deposited with 10 cycles of TMA and D_2O ALD on H/Si(111). The absorption spectrum associated with this Al_2O_3 film, referenced to H/Si (111), is shown in the inset of Fig. 5. The negative peak at 2083 cm^{-1} indicates that all the hydrogen is removed upon Al_2O_3 growth (TMA/D_2O exposures at 300°C). The broad peak centered at 920 cm^{-1} corresponds to the Al_2O_3 phonon mode confirming the formation of an Al_2O_3 thin film (12). The shoulder at ~1100 cm^{-1} is due to the interfacial Si oxide bonds.

Copper is deposited on the Al_2O_3 through a series of ALD cycles (up to 6) as shown in Fig. 5. Similar to what is observed on the Si oxide surface, a broad negative peak centered at 940 cm^{-1} is observed upon the first dose of the $[Cu(^sBu\text{-}amd)]_2$ precursor. This feature corresponds to the Al_2O_3 LO phonon of the thin film, due to chemical interaction of the precursor with the surface. After H_2 dosing, this absorbance feature is partially recovered, as evidenced by a positive band at the same spectral position in the differential spectrum labeled 1 cycle. The same trend is observed for the subsequent cycles, up to the 6^{th} H_2 dose. These observations are consistent with the coverage of Al_2O_3 upon exposure to the Cu precursor, involving a chemical interaction between the oxide and the precursor, and subsequent agglomeration upon H_2 exposure indicating that the Cu atoms can diffuse once their ligands are removed. RBS measurements show that the growth rate on this Al_2O_3 film is ~ 0.2 Å per cycle, which is lower than that of the initial deposition on Si oxide surface.

During the first 3 cycles, there is a large increase (and partial decrease during H_2 exposure) of CH_x stretching mode visible in the 2800 cm^{-1}-3000 cm^{-1} range. It is also noticeable that for the 6^{th} dosing of precursor (5.5 cycle), the change of CH_x group is very small which may indicate a slower growth rate comparing with the first several cycles. The variation

of the features at 1606 cm^{-1} and 1509 cm^{-1} is also interesting and may relate to C and N bond in the ligand of the precursor. These modes are still under investigation.

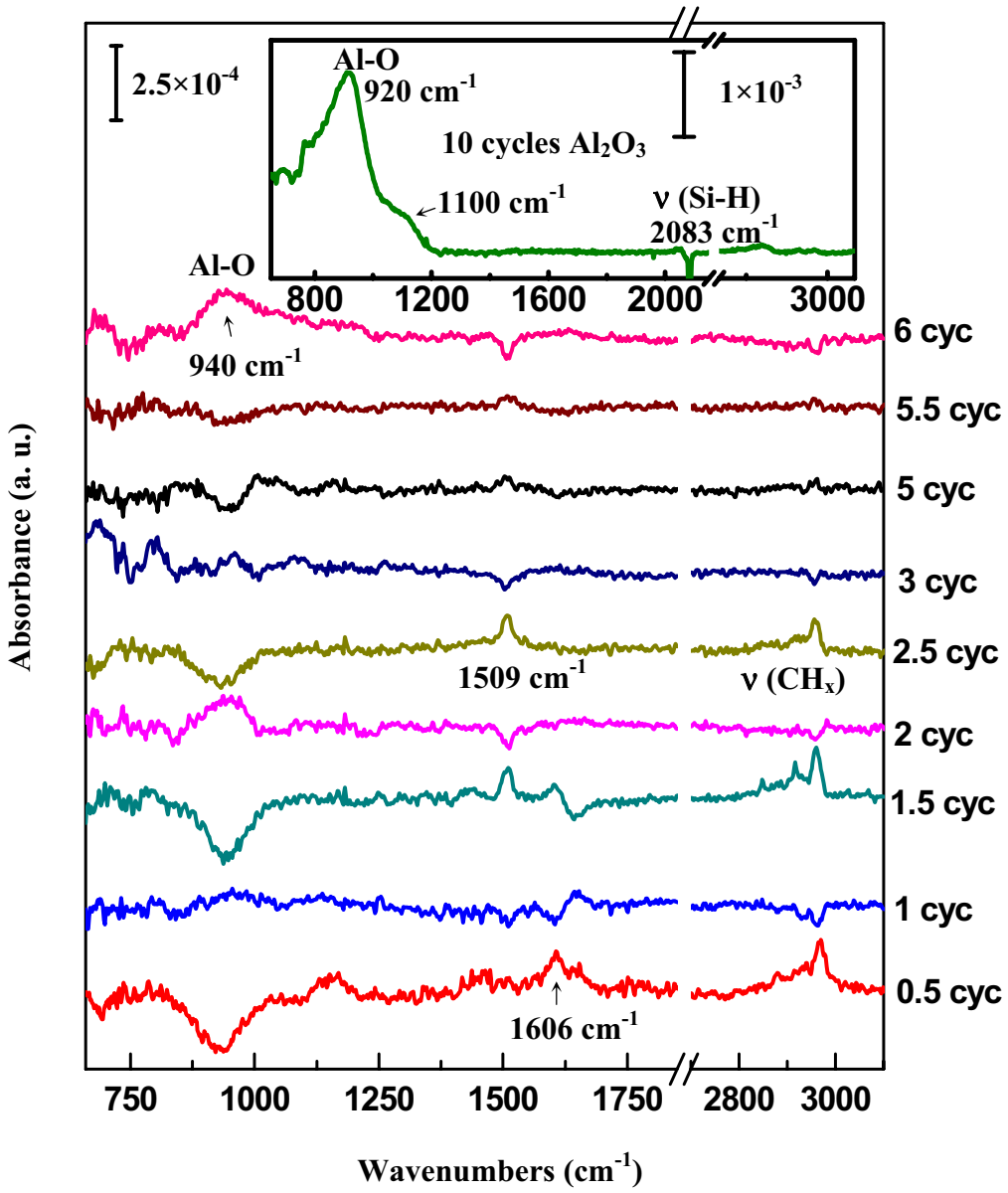

Fig. 5 Differential FTIR absorption spectra of 6 cycles (H_2 dosing after Cu(^{s}Bu-amd)]$_2$) copper ALD on Al_2O_3. Each spectrum is referenced to the previous surface and the 0.5 cycle is referenced to Al_2O_3 starting surface. Each 0.5 cycle is Cu precursor dosing and full cycle is ended by H_2 dosing. The inset is the 10 cycles Al_2O_3 starting surface referenced to H/Si (111) surface.

Si nitride surface

Silicon nitride is a very good insulator and diffusion barrier against oxygen, water and dopants diffusion. It is also a very important starting surface for depositing copper. It can

be obtained by many methods such as sputtering or PECVD. We have used here thermal nitridation by NH_3 because it is highly compatible with ALD processing and suitable to grow a thin layer of silicon nitride (< 1nm).

The spectrum associated with the nitrided, grown on H/Si (100), is shown in the inset of Fig. 6. The spectrum is referenced to the H/Si (100) surface. The negative band around 2100 cm^{-1} indicates the loss of all Si-H during the nitridation at 600°C. A peak centered at 1547 cm^{-1} is associated with the scissor mode of NH_2 (13). The SiN_x phonon modes (TO/LO) are observed at 840 cm^{-1} and 1058 cm^{-1} showing the formation of a SiN_x layer (14, 15). A noticeable peak centered at 936 cm^{-1} may be caused by the loss of Si-H_2 (di-hydride scissor mode).

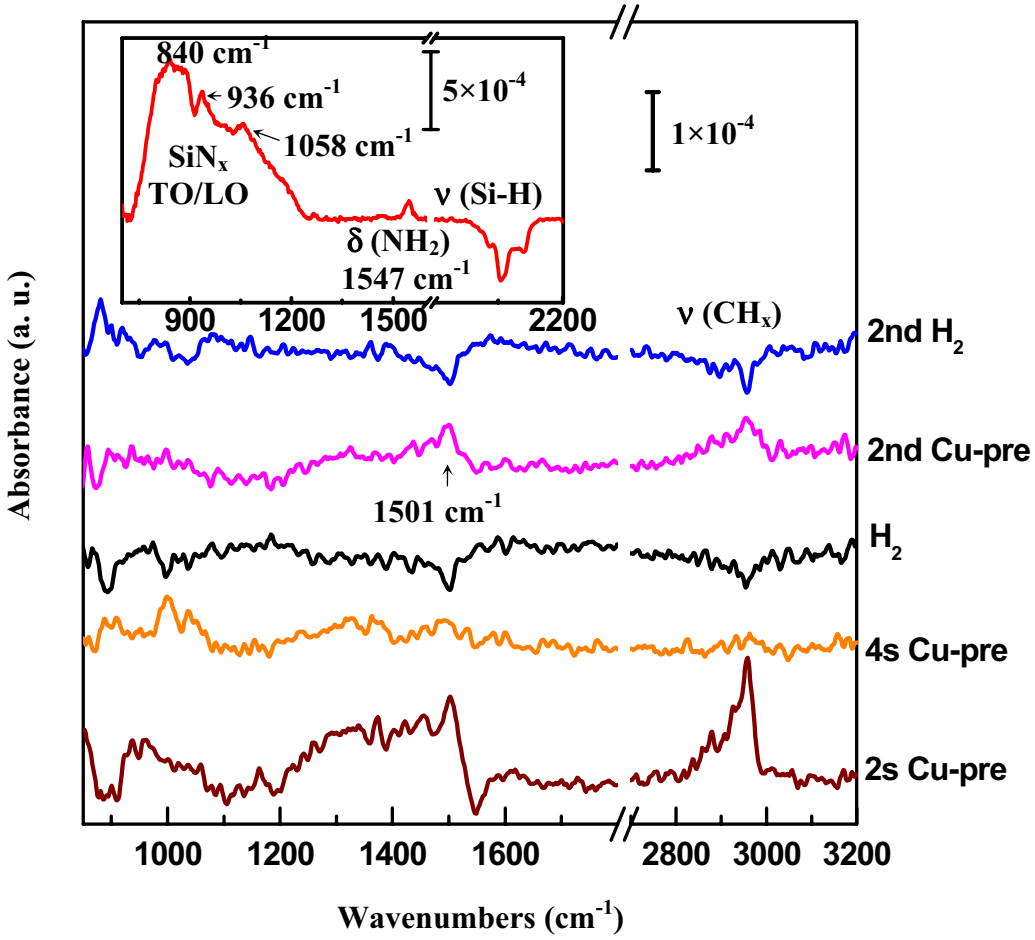

Fig. 6 Differential FTIR absorption spectra of 2 cycles (H_2 dosing after Cu(^{s}Bu-amd)]$_2$) copper on SiN_x. Each spectrum is referenced to that of the previous surface and the 0.5 cycle is referenced to the SiN_x starting surface. Each 0.5 cycle corresponds to a pulse of Cu precursor and each full cycle is ended by a H_2 pulse. The inset is the spectrum of the SiN_x starting surface referenced to the H/Si (100) surface.

Fig. 6 summarizes the differential spectra associated with each half cycle for a total of two full cycles of copper deposition on a nitrided surface. The first two spectra are recorded after two exposures to the metal precursor alone, the first for 2s, and the second

for an additional 2s (i.e. 4s in total). The relatively featureless second spectrum indicated that saturation coverage was reached with a 2s pulse. In contrast to the SiO_2 and Al_2O_3 surfaces, there are no noticeable variations in the spectral range corresponding to the SiN_x phonons (840 and 1060 cm^{-1}). This observation indicates that Cu diffusion on nitride may be harder, reducing agglomeration at the growth temperature. RBS measurements show that the growth rate on nitride is ~ 0.35 Å per cycle, which is lower than that of the initial deposition on Si oxide surfaces but higher than on Al_2O_3 surfaces.

There is again a cyclical variation of the CH_x stretching modes (increase upon copper precursor exposure, and decrease upon H_2 exposure), consistent with the expected reaction between the absorbed precursor ligands and H_2. Again the mode around 1501 cm^{-1} shows an interesting behavior as on Al_2O_3 surfaces, which may have the same origin.

Conclusion

Using both *in situ* FTIR and RBS measurement, the growth of Cu films using ALD with $[Cu(^{s}Bu\text{-}amd)]_2$ precursor and H_2 has been shown to exhibit marked difference on surfaces that are functionalized differently. The H/Si surface shows the least growth rate. The oxide surface gives the highest initial growth rate with a substantial decrease once some Cu is deposited. Variations in the intensity of the SiO_x and Al_2O_3 phonon modes during ALD growth are consistent with an initial uniform chemical interaction between the metal precursor and the oxide surfaces and subsequent Cu agglomeration upon H_2 reduction. Such agglomeration is not observed for Cu films on nitrided silicon surface.

Acknowledgments

This work was supported by the National Science Foundation (grant CHE-0415652).

References

1. C. M. Whelan, M. Kinsella, L. Carbonell, H. M. Ho and K. Maex, *Micorelectron Eng.,* **70**, 551 (2003)
2. M. -T. Ho, Y. Wang, R. T. Brewer, L. S. Wielunski, Y. J. Chabal, N. Moumen, and M. Boleslawski, Appl. Phys. Lett., **87**, 133103 (2005)
3. D. Hausmann, J. Becker, S. Wang, and R. G. Gordon, *Science*, **298**, 402 (2002)
4. B. S. Lim, A. Rahtu, and R. G. Gordon, *Nat. Matt.*, **2,** 749 (2003)
5. C. Musgrave and R. G. Gordon, *Future Fab International*, **18**,126 (2005)
6. P. Martensson and J. O. Carlsson, *J. Electrochem. Soc.,*, **145**, 2926 (1998)
7. M. Juppo, M. Ritala, and M. Leskela, *J. Vac. Sci. Technol. A*., **A15**, 2330 (1997)
8. A.U. Mane and S. A. Shivashankar, *J. Cryst. Growth*, **275**, e1253 (2005)
9. Z. Li, A. Rahtu, and R. G.Gordon, *J. Electrochem. Soc.,*, **153**, C787 (1998)

10. Y. J. Chabal, G. S. Higashi, K. Raghavachari, and V. A. Burrows. *J. Vac. Sci. Technol. A*, **7**, 2104 (1989)
11. K. T. Queeney, N. Herbots, J. M. Shaw, V. Atluri, Y. J. Chabal, *Appl. Phys. Lett.*, **84**, 493 (2004)
12. M. Frank, Y. J. Chabal and G. D. Wilk, *Appl. Phys. Lett.*, **82**, 4758 (2003).
13. K. T. Queeney, K. Raghavachari and Y. J. Chabal, *Phys. Rev. Lett.*, **86**, 1046 (2001)
14. G. Dupont, H. Caquineau, B. Despax, R. Berjoan, and A. Dollet, *J. Phys. D: Appl. Phys.*, **30**, 1064 (1997)
15. Y. Wang, M. Dai, S. Rivillon, M-T. Ho, and Y. J. Chabal, *SPIE Proceedings*, **6325**, 63250G (2006)